RC22691 (W0301-032) January 7, 2003
OTHER

IBM Research Report

Thin Strain-relaxed SiGe buffer Layers with Low Threading Dislocation Density and Surface Roughness

Silke Christiansen, Patricia M. Mooney, Jack O. Chu, Alfred Grill
IBM Research Division
Thomas J. Watson Research Center
P.O. Box 218
Yorktown Heights, NY 10598

Research Division
Almaden - Austin - Beijing - Delhi - Haifa - India - T. J. Watson - Tokyo - Zurich

LIMITED DISTRIBUTION NOTICE: This report has been submitted for publication outside of IBM and will probably be copyrighted if accepted for publication. It has been issued as a Research Report for early dissemination of its contents. In view of the transfer of copyright to the outside publisher, its distribution outside of IBM prior to publication should be limited to peer communications and specific requests. After outside publication, requests should be filled only by reprints or legally obtained copies of the article (e.g. , payment of royalties). Copies may be requested from IBM T. J. Watson Research Center , P. O. Box 218, Yorktown Heights, NY 10598 USA (email: reports@us.ibm.com). Some reports are available on the internet at http://domino.watson.ibm.com/library/CyberDig.nsf/home .

Thin strain-relaxed $Si_{1-x}Ge_x$ buffer layers with low threading dislocation density and surface roughness

S.H. Christiansen, P.M. Mooney, J.O. Chu and A. Grill

IBM Semiconductor Research and Development Center,

Research Division, T.J. Watson Research Center, Yorktown Heights, NY 10598 USA

Abstract

Relaxed $Si_{1-x}Ge_x$ layers serve as 'virtual substrates' for strained Si devices. By means of He^+-ion implantation and annealing we have achieved strain-relaxed $Si_{1-x}Ge_x$ (x=0.15 - 0.21) layers less than 500 nm thick with a threading dislocation density typically $<2x10^5$ cm^{-2}, comparable to the lowest published values for graded SiGe buffer layers. The root mean square (RMS) surface roughness is less than 0.8 nm, about an order of magnitude lower than for graded SiGe buffer layers. As much as ~85% of the lattice mismatch strain is relieved, depending on the thickness of the SiGe layer. After He^+ implantation into the Si(001) substrate below a strained SiGe layer grown by ultra-high vacuum chemical vapor deposition (UHVCVD), platelets that emit prismatic dislocation loops are formed below the Si/SiGe interface during subsequent annealing. These dislocations glide towards the interface where they break, and glide further to form a misfit dislocation network that contributes to strain relaxation. A novel method to determine threading dislocation densities in these samples using atomic force microscopy is also discussed.

$Si/Si_{1-x}Ge_x$ virtual substrates are used for strained Si devices to exploit the enhanced carrier mobility from tensile strain in the Si channel [1-4]. It is important both to achieve sufficient strain relaxation in the $Si_{1-x}Ge_x$ buffer layer so that the material will not change upon subsequent processing steps and to obtain a low density of threading dislocations, which degrade device performance, despite the high density of misfit dislocations that are needed for strain relaxation. In state-of-the-art graded buffer layers the misfit dislocations are confined to the lower part of the graded buffer layer and the Si substrate [5-10]. The threading dislocation density is in the range 10^5-10^8 cm^{-2}, depending on the final alloy composition and the grading rate of the buffer layer. More importantly, the threading dislocations are inhomogeneously distributed. Rows of threading dislocations form along pile-ups of misfit dislocations that arise from the operation of Frank-Read multiplication sources [7-8]. These dislocation pileups result in a cross-hatch surface pattern with RMS surface roughness values as high as 25 nm [9-11]. The lowest density of threading dislocations has been found for very slow grading rates [7,8], i.e., for graded layers that are several micrometers thick. However, growing such thick layers is a poor option for device applications, since $Si_{1-x}Ge_x$ has a relatively low heat conductivity and epitaxial growth is costly.

It has been shown that He^+ implantation into the Si substrate through fully strained, metastable $Si_{1-x}Ge_x$ layers ($x<0.3$) and subsequent annealing effectively promotes strain relaxation [12-15]. For selected implantation conditions, the He agglomerates upon annealing and forms over-pressurized cavities (platelets) that serve as dislocation nucleation sources [15]. Prismatic dislocation loops nucleate at these platelets and glide towards the $Si/Si_{1-x}Ge_x$ interface where they break, and further glide to relieve mismatch

strain in the $Si_{1-x}Ge_x$ layer. In this paper we will demonstrate the application of ion implantation and annealing to control strain relaxation of $Si_{1-x}Ge_x$ layers with $0.15<x<0.21$ to obtain a homogeneous distribution of threading dislocations at a density typically $<2\text{x}10^5$ cm^{-2} and a root mean square (RMS) surface roughness <0.8 nm. This threading dislocation density is comparable to the lowest published values for graded $Si_{1-x}Ge_x$ buffer layers.

Fully strained $Si_{1-x}Ge_x$ layers having $0.15<x<0.21$ and thickness <500 nm were grown epitaxially by ultra-high vacuum chemical vapor deposition (UHVCVD). He^+ was implanted with the energy chosen so that the peak of the projected range of the He atoms was >100 nm below the $Si_{1-x}Ge_x$/Si interface. The values for the ion implantation energy were determined from SRIM simulations [16]. An incidence angle of 7^0 was used to avoid channeling of the He^+ ions. The implant dose selected is well below the Smart-Cut dose [17]. Annealing was carried out in a He or N_2 atmosphere at temperatures >750 ^oC for more than an hour. Atomic force microscopy (AFM), high-resolution x-ray diffraction (HRXRD) and transmission electron microscopy in planar view (PVTEM) and cross section (XTEM) were used to evaluate the samples to determine the surface roughness, degree of relaxation and defect densities.

All of the thin, <200 nm, as-grown $Si_{1-x}Ge_x$ layers are pseudomorphic. HRXRD measurements show strong interference fringes and no detectable strain relaxation. However, some of the thicker layers show weaker interference fringes and a small degree, <5%, of strain relaxation. AFM micrographs of the thicker layers show some straight lines that are surface steps originating from 60^0 misfit dislocations. As an example, Fig. 1(a)

shows the surface of a 256nm $Si_{0.81}Ge_{0.19}$ as-deposited layer. AFM images of the thinner layers show fewer misfit dislocations, or none at all, in scanned areas of comparable size. After implantation and annealing, strain relaxation of the $Si_{1-x}Ge_x$ layers occurs as is indicated by the high density of misfit dislocation lines in Fig. 1(b), which is an image of the surface of the same 256 nm-thick layer. This surface is typical of all the implanted layers after annealing, i.e. after substantial strain relaxation. The degree of relaxation after implantation and annealing increases with the thickness of the initial strained $Si_{1-x}Ge_x$ layer thickness, as is shown in Fig. 2, which also shows that regions of the same wafer that were not implanted are significantly less relaxed after annealing.

All these implanted and annealed SiGe layers relax by the same mechanism, i.e. by prismatic loop nucleation at He-induced platelets and subsequent glide of the loops to and in the $Si/Si_{1-x}Ge_x$ interface. The density of platelets is of the order of 5-10 x 10^8 cm^{-2} as shown in Fig. 3. This is a high enough density so that each platelet emits only few dislocation loops in the eight equivalent <110>-directions; thus, relaxation occurs primarily by single misfit dislocations, rather than dislocation multiplication. That this relaxation mechanism produces single dislocations is seen clearly in PVTEM micrographs at magnifications higher than the micrograph in Fig. 3. Such images are shown in Ref. 15, where details of the dislocation introduction mechanism are also discussed. Fig. 1(c) shows an AFM line scan across the surface of a 256nm-thick, relaxed $Si_{0.81}Ge_{0.19}$ layer after annealing. Consistent with the TEM images, most of the peaks that are indicative of surface steps related to misfit dislocations at the $Si/Si_{1-x}Ge_x$ interface show feature heights (peak to valley) of <1 nm. This indicates that, rather than pronounced pileups, closely spaced, individual misfit dislocations relax the $Si_{1-x}Ge_x$ layer.

A PVTEM micrograph of the 82% relaxed, 250 nm-thick $Si_{0.85}Ge_{0.15}$ layer is shown in Fig. 4, where one threading dislocation is indicated by the arrow. About ten PVTEM pictures at a magnification of 12000x, which is usually a good magnification to have the entire picture in the same orientation with respect to the electron beam, are needed for a detection limit of $2x10^5$ cm^{-2}. Since it is difficult to get enough useful area, especially when the $Si_{1-x}Ge_x$ layer is very thin, we have developed a novel dislocation counting method. This AFM-based method works well for samples that have smooth surfaces, where the monoatomic surface steps originating from 60° misfit dislocations appear as distinct features in the AFM images. A threading dislocation is located where a surface step terminates in the field of view. This method works best when using scans that are 10μm x 10μm or smaller, where terminating surface steps are very obvious when viewing the scans on a large area computer monitor at high magnification. The experimental error of this technique is 10-20%.

To verify the accuracy of this method, we fabricated samples that have a much higher threading dislocation density by modifying the implantation conditions. Fig. 5 is an AFM image that shows 20 threading dislocations, some of which are indicated by the arrows on the micrograph. We determined a threading dislocation density of $5x10^7cm^{-2}$ for this sample using the AFM counting method and this density was verified by PVTEM analysis. In contrast, the AFM micrograph of Fig. 1(b) does not show a single corner, even within a relatively large area, thus indicating a very low threading dislocation density. The detection limits for both PVTEM and AFM corner counting are similar and depend on the total area examined. To obtain a detection limit of $2x10^5$ cm^{-2}, five AFM micrographs with a

10μm x 10μm area are taken. In selected cases when more AFM scans or an extra large transmittable area is evaluated in the TEM, threading dislocation densities below the usual detection limit can be obtained, e.g., $0.4 x 10^5$ cm^{-2}.

Although the degree of relaxation is much greater for thicker layers, the threading dislocation density is essentially the same as for the thinner layers. As shown in Table I, it is in the range 0.4–$6x10^5$ cm^{-2} as measured both by PVTEM and by AFM, comparable to the best graded SiGe buffer layers. All samples with a threading dislocation density marked $<2x10^5 cm^{-2}$ in Table 1 have a threading dislocation density below the usual detection limit of these measurement techniques. Interestingly, a threading dislocation density below the detection limit is found for some of the thicker, most highly relaxed layers. The low density of threading dislocations, even in thicker samples having a few dislocation pile-ups as shown in Fig. 1, suggests that, in contrast to graded buffer layers [18], dislocation blocking [19,20] is not a major problem in these implanted and annealed buffer layers. We note, however, that there is scatter in the data. The highest threading dislocation density, $6x10^5$ cm^{-2}, was found for a 188 nm-thick $Si_{0.79}$ $Ge_{0.21}$ layer. The difference between this layer and other thicker layers that have a lower threading dislocation density is that the initial $Si_{0.79}Ge_{0.21}$ layer had a relatively high density of misfit dislocation pileups, each containing many dislocations. Thus, the quality of the initial pseudomorphic $Si_{1-x}Ge_x$ layer is critical for achieving a low threading dislocation density after He^+-implantation and annealing.

In summary, we have investigated the effectiveness of He^+-implantation and annealing for the relaxation of strained $Si_{0.84}Ge_{0.16}$ and $Si_{0.80}Ge_{0.20}$ layers on Si(001)

substrates. The thicker the layer, the higher the degree of relaxation; for example, 97nm thick $Si_{0.82}Ge_{0.18}$ layers are only ~37% relaxed, whereas 334 nm-thick $Si_{0.81}Ge_{0.19}$ layers are 83% relaxed. The RMS surface roughness is below 0.8 nm for all layers, about an order of magnitude lower than for graded buffer layers. The threading dislocation density is typically $<2x10^5$ cm^{-2}, which is the usual detection limit of the counting techniques used. This threading dislocation density is two orders of magnitude lower than previously published values for implanted/annealed $Si_{1-x}Ge_x$/Si layers obtained by a similar method [13,14] and comparable to the best published values for graded buffer layers [5-10]. The key to the improved properties of our implanted and annealed layers is the good quality of the initial strained $Si_{1-x}Ge_x$ layer. Implantation and annealing provides for dislocation nucleation sources that are more or less uniformly distributed across the wafer. Thus, single dislocations are observed rather than the dislocation pile-ups that are found in graded $Si_{1-x}Ge_x$ buffer layers.

The authors are grateful for the use of electron microscopes at the University of Erlangen-Nuremberg (Prof. H.P. Strunk). S.H.C. was partially supported by a Feodor Lynen Fellowship awarded by the Alexander von Humboldt Foundation. We also gratefully acknowledge D.L. Lacey for assistance with XRD measurements and P.A. Saunders for He^+ implants.

References:

1. B.S. Meyerson, Proc. IEEE **80**, 1592 (1992).
2. K. Ismail, S. Rishton, J.O. Chu and B.S. Meyerson, Electron Device Letters **14**, 348 (1993).
3. U. Konig, Mat. Res. Soc. Symp. Proc. **533**, 3 (1998).
4. K. Rim, J.L. Hoyt and L.F. Gibbons, IEEE Trans. Electron Devices **47**, 1406 (2000).
5. F.K. LeGoues, B.S. Meyerson, J.F. Morar, Phys.Rev.Lett. **66**, 2903 (1991).
6. F.K. LeGoues, B.S. Meyerson, J.F. Morar, P.D. Kirchner, J. Appl. Phys. **71**, 4230 (1992).
7. E.A. Fitzgerald, Y.H. Xie, D. Monroe, P.J. Silverman, J.M. Kuo, A.R. Kortan, F.A. Thiel, B.E. Weir, J. Vac. Sci. Technol. B**10**, 1807 (1992).
8. P.M. Mooney, Materials Science and Engineering Reports **R17**, 105 (1996), and references therein.
9. D.J. Wallis, D.J. Robbins, A.J. Pidduck, G.M. Williams, A. Churchill and J. Newey, Mat. Res. Symp. Soc. 533, 77 (1998).
10. D.J. Robbins, J.L. Glasper, D. Wallis, A.C. Churchill, A.J. Pidduck and W.Y. Leong, in *Lattice Mismatched Thin Films*, Ed. E.A. Fitzgerald (The Minerals, Metals, & Materials Society, Warrendale, PA, 1999) pp. 3-11.
11. M.A. Lutz, R.M. Feenstra, F.K. LeGoues, P.M. Mooney and J.O. Chu, Appl. Phys. Lett. 66, 724 (1995).
12. D.M. Follstaedt, S.M. Myers, S.R. Lee, Appl. Phys. Lett. **69**, 2059 (1996).
13. S. Mantl, B. Hollaender, R. Liedtke, S. Mesters, H.J. Herzog, H. Kibbel, T. Hackbarth, Nucl. Instr. and Meth. B**147**, 29 (1999);

14. M. Luysberg, D. Kirch, H. Trinkaus, B. Hollaender, S. Lenk, S. Mantl, H.J. Herzog, T. Hackbarth, P.F. Fichtner, J. Appl. Phys. 92, 4295 (2002).

15. S.H. Christiansen, P.M. Mooney, J.O. Chu, A. Grill, Mat. Res. Soc. Symp. Proc. **686**, 3 (2002).

16. J.F. Ziegler, J.P. Biersack, U. Littmark, *The stopping and Range of Ions in Solids* (Pergamon, New York, 1985).

17. M. Bruel, Nucl. Instr. and Meth. B**108**, 313 (1996).

18. E.A. Fitzgerald, M.T. Bulsara, M.T. Currie, S.B. Samavedam and T.A. Langdo, in *Lattice Mismatched Thin Films*, Ed. E.A. Fitzgerald (The Minerals, Metals, & Materials Society, Warrendale, PA, 1999) pp. 63-71.

19. K.W. Schawrz and J. Tersoff, Appl. Plys. Lett. 69, 1220 (1996).

20. E.A. Stach, K.W. Schwarz, R. Hull, F.M. Ross and R.M. Tromp, Phys. Rev. Lett. 84, 947 (2002).

Table I. Degree of relaxation, surface roughness and threading dislocation density in implanted and annealed $Si_{1-x}Ge_x$ layers. The uncertainty in the degree of relaxation is ±2%, in the alloy composition is ±0.05 and in the dislocation count is ~20%. The $Si_{1-x}Ge_x$ layer thickness was measured by XRD prior to strain relaxation. The threading dislocations were counted using AFM micrographs[a] and, for selected samples, also by PVTEM[b].

alloy composition, x	layer thickness [nm]	strain relaxation [%]	RMS roughness [nm]	threading dislocation density [$\times 10^5$ cm^{-2}]
0.15	250	82	0.62	2.0[a,b]
0.15	460	86	0.60	0.8[a,b]
0.17	101	47	0.29	2-3[a]
0.19	97	46	0.39	<2.0[a]
0.19	170	70	0.40	<2.0[a,b]
0.19	256	84	0.52	<2.0[a,b]
0.19	334	90	0.79	<2.0[a,b]
0.21	110	64	0.28	0.4[a]
0.21	188	75	0.47	6.0[a,b]

Figure Captions:

Fig. 1. AFM micrographs of a 256nm-thick $Si_{0.81}Ge_{0.19}$ buffer layer: (a) as-grown with a few misfit dislocations visible by their surface steps and (b) after ion implantation and annealing with a dense network of single misfit dislocation related surface steps. The ridges (white), due to local roughness peaks in the relaxed layer, reside where misfit dislocations where already existent in the as grown layer. (c) Topology along a line scan across the surface perpendicular to one set of misfit dislocations and parallel to the other; the arrow indicates a dislocation pile-up which is also marked in (b).

Fig. 2. The degree of strain relaxation in $Si_{0.84}Ge_{0.16}$ (squares) and $Si_{0.80}Ge_{0.20}$ (circles) layers with (solid symbols) and without (open symbols) He^+ implants after annealing at 800^oC for 2 hrs.

Fig. 3. Planar view transmission electron micrograph, taken under bright field multibeam conditions with the electron beam parallel to the <100>-direction, of an implanted and annealed 97 nm-thick $Si_{0.85}Ge_{0.15}$ layer on Si(001). One can see the network of 60° misfit dislocations at the $Si/Si_{0.85}Ge_{0.15}$ interface together with platelets below the interface (round, dark features) at a density of $5\text{-}10x10^8$ cm^{-2}.

Fig. 4. Planar view transmission electron micrograph of an implanted and annealed 250 nm-thick $Si_{0.85}Ge_{0.15}$ layer on Si(001). The misfit dislocation network at the $Si/Si_{0.75}Ge_{0.15}$ interface is visible in some areas; in others the interface was thinned away during sample

preparation, so that only the $Si_{0.75}Ge_{0.15}$ layer is present. A threading dislocation is indicated by the white arrow.

Fig. 5. AFM micrograph of a sample with a high density of threading dislocations illustrating the AFM method for counting threading dislocations. Some threading dislocations are indicated by the arrows.

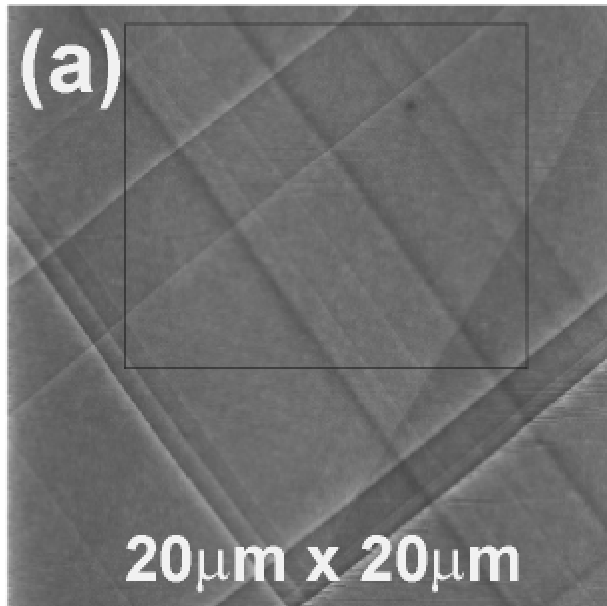

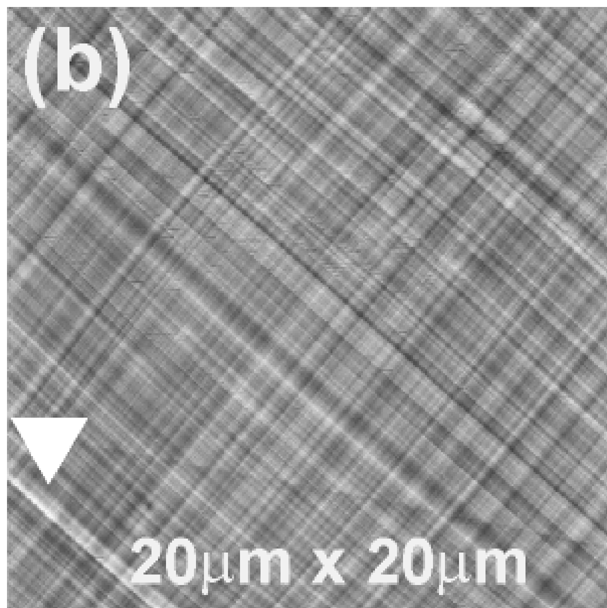

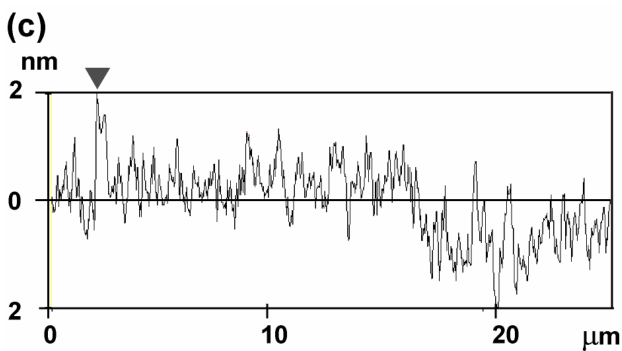

Fig. 1. AFM micrographs of a 256nm-thick $Si_{0.81}Ge_{0.19}$ buffer layer: (a) as-grown with a few misfit dislocations visible by their surface steps and (b) after ion implantation and annealing

with a dense network of single misfit dislocation related surface steps. The ridges (white), due to local roughness peaks in the relaxed layer, reside where misfit dislocations where already existent in the as grown layer. (c) Topology along a line scan across the surface perpendicular to one set of misfit dislocations and parallel to the other; the arrow indicates a dislocation pile-up which is also marked in (b).

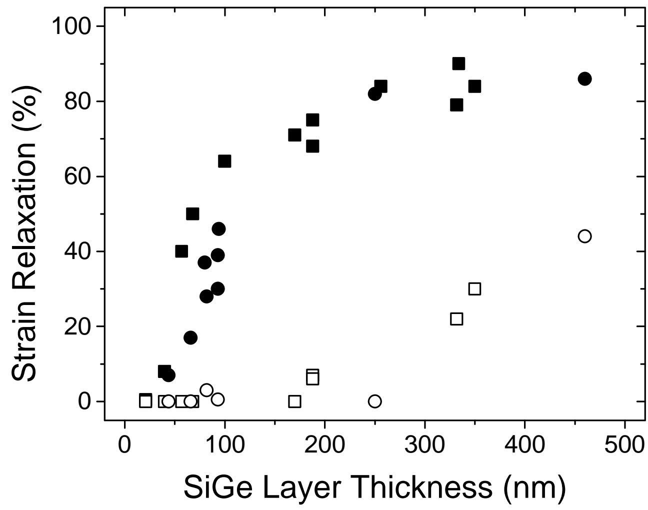

Fig. 2. The degree of strain relaxation in $Si_{0.84}Ge_{0.16}$ (squares) and $Si_{0.80}Ge_{0.20}$ (circles) layers with (solid symbols) and without (open symbols) He^+ implants after annealing at 800°C for 2 hrs

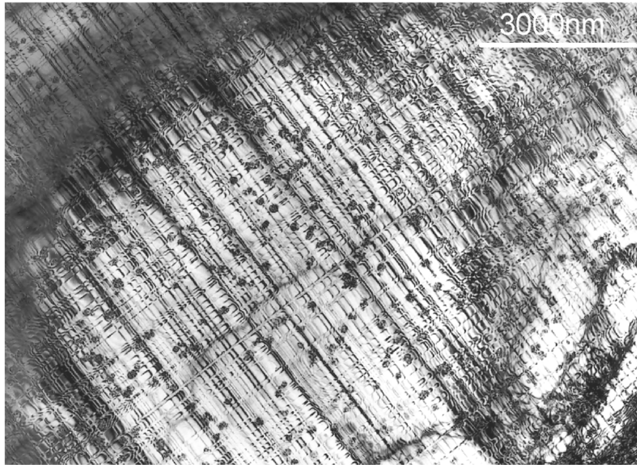

Fig. 3. Planar view transmission electron micrograph, taken under bright field multibeam conditions with the electron beam parallel to the <100>-direction, of an implanted and annealed 97 nm-thick $Si_{0.85}Ge_{0.15}$ layer on Si(001). One can see the network of 60° misfit dislocations at the $Si/Si_{0.85}Ge_{0.15}$ interface together with platelets below the interface (round, dark features) at a density of 5-10x10^8 cm^{-2}.

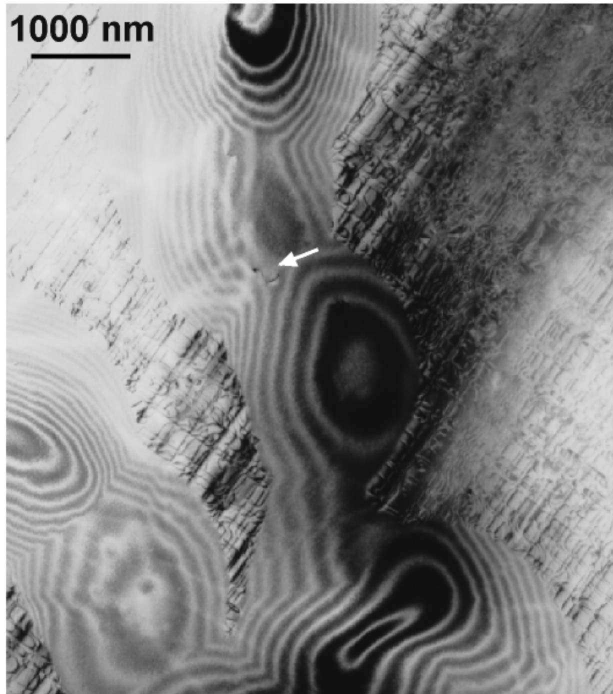

Fig. 4. Planar view transmission electron micrograph of an implanted and annealed 250 nm-thick $Si_{0.85}Ge_{0.15}$ layer on Si(001). The misfit dislocation network at the $Si/Si_{0.75}Ge_{0.15}$ interface is visible in some areas; in others the interface was thinned away during sample preparation, so that only the $Si_{0.75}Ge_{0.15}$ layer is present. A threading dislocation is indicated by the white arrow.

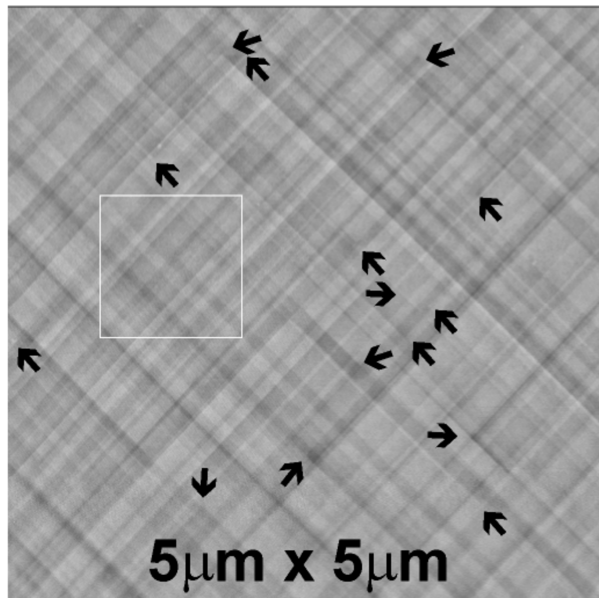

Fig. 5. AFM micrograph of a sample with a high density of threading dislocations illustrating the AFM method for counting threading dislocations. Some threading dislocations are indicated by the arrows.